# Ship detection using GNSS-Reflectometry in backscattering configuration

A. Di Simone, P. Braca, L. M. Millefiori
NATO Science and Technology Organization Centre for Maritime Research and Experimentation (STO CMRE)
La Spezia, Italy
{alessio.disimone, paolo.braca, leonardo.millefiori}@cmre.nato.int

P. Willett
School of Engineering
University of Connecticut
Storrs, CT, USA
peter.willett@uconn.edu

***Abstract*—The chance of exploiting the Global Navigation Satellite Systems-Reflectometry (GNSS-R) remote sensing technology in the field of maritime surveillance and ship traffic monitoring has been explored in the very recent past. The conventional bistatic GNSS-R is based on the acquisition of GNSS navigation messages in a forward-scattering geometry, where the investigated region surrounds the specular reflection point. The peculiarities of the ship detection problem, where man-made dihedral structures come into play, make the conventional configuration unsuitable for such an application, especially from spaceborne platforms. Very recently, the backscattering configuration has been demonstrated to greatly enhance the presence of targets within GNSS-R delay-Doppler maps (DDM). In this paper, a thorough comparison of the forward- and back-scattering configurations for ship detection application from spaceborne GNSS-R instruments is presented in order to quantitatively evaluate the benefits of the backscattering configuration with respect to the conventional one. The analysis is performed by computing the signal-to-noise-plus-clutter ratio in both configurations as a function of the sea state, ship orientation and radar look angle.**

***Keywords—maritime surveillance; ship detection; GNSS-Reflectometry; bistatic radar; electromagnetic scattering***

## I. Introduction

The maritime domain plays host to fields as diverse as global economy, international security, and environment monitoring. Worldwide ship traffic and sea trades have been increasing continuously over the past five decades with tons loaded increased from 4,000 millions in 1990 to about 10,000 millions in 2015 [1]. The world fleet grew by 3.5% in 2015, representing the lowest annual growth rate in over a decade [1]. Illegal fishery activities have severe adverse impacts on the sustainable fisheries, marine ecosystems and socioeconomic development [2]. It is estimated that about 70% of the world's fish stocks are fully exploited or in a state of collapse [2]. Illegal migration, piracy, drug smuggling, counter-terrorism, and foreign military activities partly represent the range of issues arising in the detection and tracking of maritime assets.

A number of technologies and remote sensing tools have been designed or exploited for detecting and monitoring targets over the sea surface. The Automatic Identification System (AIS) is a shipborne self-reporting system that enables vessels to broadcast their position and other voyage-related (name, speed, route) information. AIS receiving networks can be terrestrial or spaceborne. This protocol requires AIS facilities installed onboard, and, therefore, only cooperating ships can be monitored [3]. The new-generation spaceborne optical and synthetic aperture radar (SAR) systems enable the detection of ships up to few meters long worldwide, owing to global coverage capabilities and high-resolution imagery [4], [5]. However, both technologies provide imagery with limited revisit time (up to 12 hours for the Cosmo-SkyMed constellation), thus preventing continuous real-time sea traffic monitoring on a global scale [6], [7].

Global Navigation Satellite System-Reflectometry (GNSS)-Reflectometry exploits GNSS signals reflected off the Earth's surface to infer about geophysical parameters of the sensed scene, such as wind speed, sea surface height and sea state [8], [9], [10]. It was first used in the late 1980s for scatterometry applications [11]. Among other applications, such as ocean topography [12], oil slick detection [13], and tsunami detection [14], the chance of exploiting Earth-reflected GNSS signals for sea target detection has been investigated in the recent past and a few literature exists [15-19]. In [15] an automatic algorithm for the detection of large sea targets, i.e., large vessels, sea ice sheets, from GNSS-R delay-Doppler map (DDM) is presented and tested using actual TechDemo Sat (TDS)-1 data. It is based on the estimation and suppression of the sea clutter in the DDM finalized to the detection of the secondary peaks due to the large targets. However, important issues for the target detection arise with the conventional forward-scattering configuration [18]. They are discussed in the following section. The paper is organized as follows: Section II introduces the methodology used for a thorough comparison of the conventional forward-scattering and the backscattering geometric configurations. Numerical results are provided in Section III and the main conclusions are drawn in Section IV.

## II. THE IMPACT OF THE ACQUISITION GEOMETRY ON SHIP DETECTABILITY

The conventional GNSS-R acquisition process provides a DDM of a region surrounding the specular reflection point, the so-called glistening zone. This geometric configuration is also referred to as forward-scattering geometry and represents the usual configuration in GNSS-R remote sensing. Due to the strong sea clutter in the specular direction, first applications of GNSS-R in the maritime domain have been limited to the analysis of the sea surface and sea state [8-12]. However, as also discussed in [18], several issues arise for target detection application from delay-Doppler Map (DDM) using the conventional forward-scattering acquisition geometry.

First, the target echo appears as a weak secondary peak in the DDM [15], [18], [20], unless the ship is perfectly located in the specular reflection point. In the former case, it may be difficult to detect the target peak, unless a sea clutter suppression step is performed [15]. In the latter case, an ambiguity arises since the target return causes a strongly-peaked DDM, as in the case of a very calm sea. In this case, it would be difficult to correctly detect the target. Second, for fast-moving GNSS-R receivers, the energy reflected from the ship decreases rapidly with increasing integration time since the target energy rapidly integrates incoherently as the platform moves. Benefits in target detectability are expected if moving to the backscattering configuration, where the transmitting and receiving platforms and the target are aligned. Indeed, this configuration allows for the detection of 1) a stronger ship target echo which is reflected by the ship hull-sea surface dihedral structure in a direction depending on the ship orientation, 2) a weak sea clutter, mainly concentrated in the forward direction [21].

In order to compare the conventional forward-scattering configuration with the backscattering one, the signal-to-noise-plus-clutter ratio (SNCR) is evaluated. It is defined as:

$$SNCR = \frac{P_{r,ship}}{P_n + P_{r,sea}} \quad (1)$$

where

$$P_{r,ship} = P_t G_t G_r \frac{1}{(4\pi)^3} \left( \frac{\lambda \cos\vartheta \cos\vartheta_s}{h_t h_r} \right)^2 \sigma_{ship}(\vartheta, \vartheta_s, \varphi_s, \alpha, \varphi) \quad (2)$$

$$P_{r,sea} = P_t G_t G_r \frac{1}{(4\pi)^3} \left( \frac{\lambda \cos\vartheta \cos\vartheta_s}{h_t h_r} \right)^2 \sigma_{sea}(\vartheta, \vartheta_s, \varphi_s, \alpha) \quad (3)$$

$$P_n = \frac{k_B T_E}{T_i} \quad (4)$$

are the target received power, sea surface received power (also referred to as sea clutter), and thermal noise power, respectively. The symbols used are listed in Table I, where values are reported assuming GPS as the transmitting GNSS and TDS-1 as the receiving GNSS-R instrument.

TABLE I. LIST OF SYMBOLS. VALUES IN SI UNITS ARE REPORTED FOR GPS AND TDS-1

| Symbol | Parameter | Value |
|---|---|---|
| $P_{r,ship}$ | Received power from ship | Variable |
| $P_{r,sea}$ | Received power from sea surface | Variable |
| $P_n$ | Noise power at the receiver | $3.12\times10^{-18}$ |
| $P_t$ | Transmitted power | 26.61 |
| $G_t$ | Transmitter antenna gain | 19.95 |
| $G_r$ | Receiver antenna gain | 25.12 |
| $\lambda$ | Signal wavelength | 0.19 |
| $h_t$ | Transmitter altitude | $2.02\times10^{7}$ |
| $h_r$ | Receiver altitude | $5.40\times10^{5}$ |
| $\sigma_{ship}$ | Radar cross section of the ship | Variable |
| $\sigma_{sea}$ | Radar cross section of sea surface | Variable |
| $k_B$ | Boltzmann constant | $1.38\times10^{-23}$ |
| $T_E$ | Noise temperature of the receiver | 225.70 |
| $T_i$ | Incoherent integration time | 1 |

Radar cross of sea surface has been evaluated according to [22], while the radar cross section of the ship is presented in [21] and accounts for the multiple bounce contributions between the ship hull and the sea surface. The geometry of the scattering problem and angles definition are sketched in Fig. 1. The ship return and the sea clutter both depend on the relative position between transmitter, receiver and target, i.e., $\vartheta$, $\vartheta_s$ and $\varphi_s$, and the sea state via the RMS slope α. Moreover, the power received from the ship also depends on the target aspect angle $\varphi$, that describes the ship orientation with respect to the transmitting station (Fig. 2). Other parameters, the most important of which are the ship size and the resolution cell, influence the SNCR [21].

The RMS slope is related to the Douglas sea state number SS, which in turn is related to the wind speed via the following equations [23]:

$$\alpha(SS) = 0.055 + 0.007SS, SS = 0,1,\ldots 8 \quad (5)$$

$$v(SS) = 1 + 2SS + \left( \frac{SS}{5.3} \right)^6 \quad (6)$$

## III. NUMERICAL RESULTS

Numerical simulations have been performed using parameters as defined in both Tables I and II. It is worth noting that here we explore the RR polarization channel, instead of the RL one conventionally exploited in GNSS-R. Indeed, it has been demonstrated that RR channel is more suitable than the RL one for ship detection applications [24].

Fig. 3 shows the SNCR in decibel (dB) as a function of the ship aspect angle for different Douglas sea states, namely SS0 (calm sea), SS4 (moderate sea), SS8 (very high sea) and assuming $\vartheta = 15°$ (Fig. 3a), and $\vartheta = 30°$ (Fig. 3b).

Assuming the ship observable if SNCR is greater than zero, target detectability greatly depends on the ship aspect angle. Thus, the dihedral structure formed by the ship hull and the sea surface reflects the impinging electromagnetic energy in the direction specular with respect to the ship hull. Consequently, in the backscattering configuration, the target is detectable only in a limited range of aspect angles. In addition, the main lobe of the energy scattered from the target increases with increasing sea surface roughness, i.e., with increasing sea state number, while the target energy peak decreases. This makes low sea states more favorable to target detection with ship facing the radar (aspect angle close to 0°, i.e., long ship side facing the radar, or 90°, i.e., short ship side facing the radar), and high sea states more favorable to detect ships in wider orientation configurations.

(b)

**Fig.** 4 shows the minimum observable ship length, i.e., the smallest ship exhibiting a SNCR greater than one, in the backscattering configuration as a function of the ship orientation, for different sea states and assuming $\vartheta = 15°$ (Fig. 4a), and $\vartheta = 30°$ (Fig. 4b). Most favorable conditions for target detectability in the backscattering configuration are with a target side facing the transmitting GNSS station. In this case, even ship targets on the order of meters overcome noise level in any sea state condition. With $\vartheta = 30°$, smaller ships can be observed with the higher sea states. However, even very large vessels are indistinguishable with aspect angles close to 45°.

TABLE II. SIMULATION PARAMETERS

| Parameter | Value |
|---|---|
| Polarization | RR |
| Frequency | 1.575 GHz |
| Spatial resolution | 10 km ×10 km |

## IV. CONCLUSIONS

In this paper, a numerical analysis has been conducted to assess the feasibility of the target detection problem using the conventional spaceborne GNSS-R forward-scattering configuration and to compare it with the backscattering one, where transmitter, receiver and target are aligned. To this aim, the SNCR has been evaluated in both configurations as a function of the ship orientation and sea state. In the analyzed scenarios, the transmitting GNSS is the GPS, and the receiving GNSS-R spaceborne platform is the U.K. TDS-1. Due to the strong sea clutter and weak ship echo in a forward-scattering configuration, ship detectability is seriously affected using the conventional bistatic configuration from spaceborne GNSS-R satellites. Conversely, in the backscattering direction sea clutter is weak, and target echo depends on its orientation. In the considered scenario, a SNCR up to about 40 dB is achieved with targets facing the transmitter, with a gain of about 80 dB with respect to the conventional configuration. Low sea states provide the most favorable conditions for detection, but high sea states are associated with a lower sensitivity against the target orientation. However, even in the backscattering geometry, ship detectability is seriously compromised with ship aspect angles close to 45°.


## ACKNOWLEDGMENT

This research has been funded by the Office of Naval Research under contract N00014-16-13157, and this support is acknowledged with thanks to J. Tague and M. Vaccaro. There is parallel support to ONR-Global.


## REFERENCES


[1] United Nations, "Review of Maritime Transport - 2015," in United Nations Conference on Trade and Development (UNCTAD), 2015.

[2] J. T. Martinsohn, “Deterring Illegal Activities in the Fisheries Sector,” Publications Office of the European Union, 2011.

[3] G. K. Hoye, T. Eriksen, B. J. Meland, and T. Narheim, “Space-based AIS for global maritime traffic monitoring,” in Proc. 7th IAA Symp. Small Satell. Earth Observ., Berlin, Germany, May 4–8, 2009.

[4] S. Brusch, S. Lehner, T. Fritz, M. Soccorsi, A. Soloviev, and B. van Schie, “Ship Surveillance With TerraSAR-X,” IEEE Trans. Geosci. Remote Sens., vol. 49, no. 3, pp. 1092-1103, Mar. 2011.

[5] P. Iervolino, R. Guida, and P. Whittaker, "A Model for the Backscattering From a Canonical Ship in SAR Imagery," IEEE J. Sel. Topics Appl. Earth Observ. and Remote Sens., vol. 9, no. 3, pp. 1163-1175, Mar. 2016.

[6] "COSMO-SkyMed Mission - COSMO-SkyMed System Description & User Guide," Italian Space Agency (ASI), [Online]. Available: http://www.e-geos.it/products/pdf/csk-user_guide.pdf. [Accessed November 7, 2017].

[7] P. Lombardo and M. Sciotti, "Segmentation-based technique for ship detection in SAR images," in IEE Proceedings - Radar, Sonar and Navigation, vol. 148, no. 3, pp. 147-159, Jun. 2001.

[8] J. Marchan-Hernandez, E. Valencia, N. Rodriguez-Alvarez, I. Ramos-Perez, X. Bosch- Lluis, A. Camps, F. Eugenio, and J. Marcello, “Sea-state determination using GNSS-R data,” IEEE Geoscience and Remote Sensing Letters vol. 7, no. 4, pp. 621–625, 2010.

[9] M. P. Clarizia, C. Ruf, P. Jales, and C. Gommenginger, “Spaceborne GNSS-R Minimum Variance Wind Speed Estimator,” IEEE Trans. Geosci. Remote Sens., vol. 52, no. 11, pp. 6829-6843, 2014.

[10] A. Rius, E. Cardellach, and M. Martín-Neira, “Altimetric Analysis of the Sea-Surface GPS-Reflected Signals,” IEEE Trans. Geosci. Remote Sens., vol. 48, no. 4, pp. 2119-2127, 2010.

[11] C. Hall and R. R. Cordey, "Multistatic Scatterometry," International Geoscience and Remote Sensing Symposium (IGARSS), pp. 561-562, 1988.

[12] M. P. Clarizia, C. Ruf, P. Cipollini and C. Zuffada, "First spaceborne observation of sea surface height using GPS-Reflectometry," Geophys. Res. Lett., vol. 43, no. 2, pp. 767-774, Jan. 2016.

[13] E. Valencia, A. Camps, H. Park, and N. Rodriguez-Alvarez, "Oil slicks detection using GNSS-R," in Proc. IEEE Int. Geosci. Remote Sens. Symp. (IGARSS), Vancouver, BC, Canada, Jul. 2011.

[14] Q. Yan and W. Huang, "Tsunami detection and parameter estimation from GNSS-R delay-Doppler map," IEEE J. Sel. Topics Appl. Earth Observ. Remote Sens., vol. 9, no. 10, 2016.

[15] A. Di Simone, H. Park, D. Riccio, and A. Camps, “Sea Target Detection Using Spaceborne GNSS-R Delay- Doppler Maps: Theory and Experimental Proof of Concept Using TDS-1 Data,” IEEE J. Sel. Topics Appl. Earth Observ. Remote Sens., vol. 10, no. 9, pp. 4237 - 4255, Sept. 2017.

[16] G. Carrie, T. Deloues, J. Mametsa and S. Angelliaume, "Ship Detection Based on GNSS Reflected Signals: An Experimental Plan," in Proc. Space Reflecto, Calais, France, 2011.

[17] Y. Lu, D. Yang, W. Li, J. Ding, and Z. Li, "Study on the New Methods of Ship Object Detection Based on GNSS Reflection," Marine Geodesy, vol. 32, no. 1, pp. 22-30, 2013.

[18] M. P. Clarizia, P. Braca, C. S. Ruf, and P. Willett, "Target detection using GPS signals of opportunity," in 18th International Conference on Information Fusion (Fusion), Washington, DC, 2015.

[19] A. Di Simone, A. Iodice, D. Riccio, A. Camps, and H. Park, "GNSS-R: A useful tool for sea target detection in near real-time," 2017 IEEE 3rd International Forum on Research and Technologies for Society and Industry (RTSI), Modena, 2017, pp. 1-6.

[20] Y. Lu, D. Yang, W. Li, J. Ding, and Z. Li, "Study on the New Methods of Ship Object Detection Based on GNSS Reflection," Marine Geodesy, vol. 32, no. 1, 2013.

[21] A. Di Simone, W. Fuscaldo, L. M. Millefiori, D. Riccio, G. Ruello, P. Braca, and P. Willett, "Analytical models for the electromagnetic scattering from isolated targets in bistatic configuration. Part I: Geometrical Optics solution," *IEEE Trans. Geosci. Remote Sens.*, unpublished.

[22] G. Franceschetti, A. Iodice, and D. Riccio, "A canonical problem in electromagnetic backscattering from buildings," IEEE Trans. Geosci. Remote Sens., vol. 40, no. 8, pp. 1787–1801, 2002.

[23] D. K. Barton, "Radar Equations for Modern Radar," 1st Edition, Artech House, cap. 9, pp. 324, 2012.

[24] A. Di Simone, L. M. Millefiori, G. Di Martino, A. Iodice, D. Riccio, G. Ruello, P. Braca, and P. Willett, "Spaceborne GNSS-Reflectometry for Ship Detection Applications: Impact of Acquisition Geometry and Polarization," 2018 IEEE International Geoscience and Remote Sensing Symposium (IGARSS), submitted.

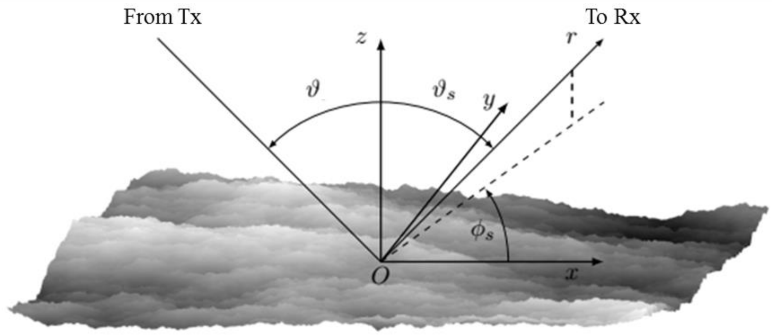


Fig. 1: Reference system of the scattering problem and angles definition.

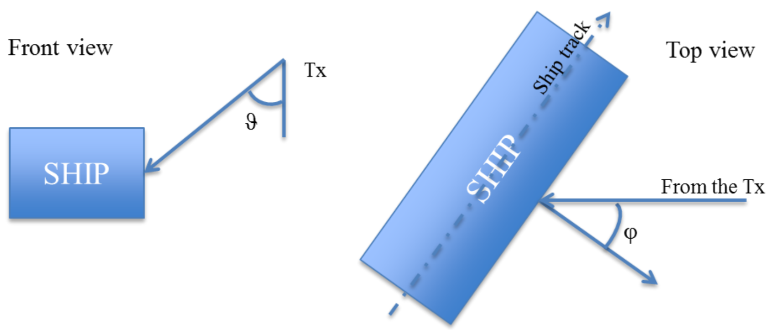


Fig. 2: Ship geometry and angles definition.

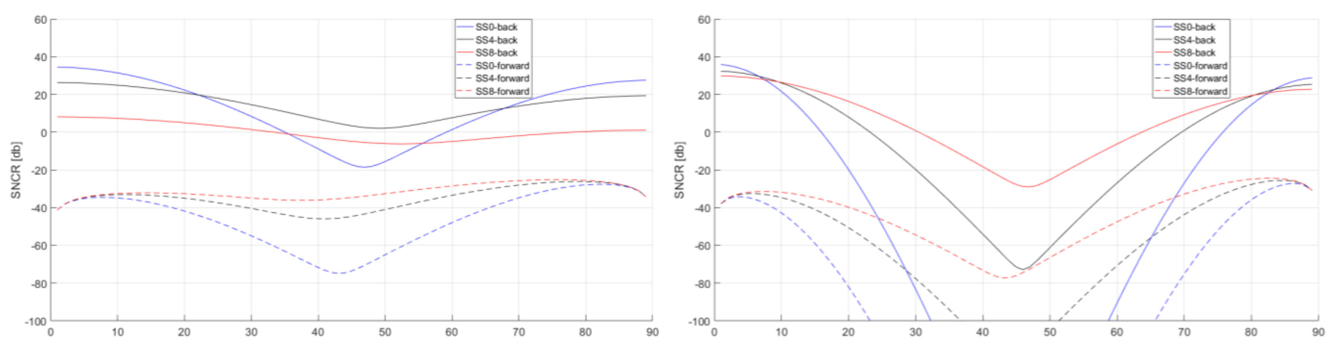


(a) (b)

Fig. 3: SNCR of the ship target as a function of the target aspect angle and for SS0 (calm sea, blue lines), SS4 (moderate sea, black lines), SS8 (very high sea, red lines) in the backscattering (solid lines) and forward scattering (dashed lines) geometric configurations. (a) $\vartheta = 15°$, (b) $\vartheta = 30°$.

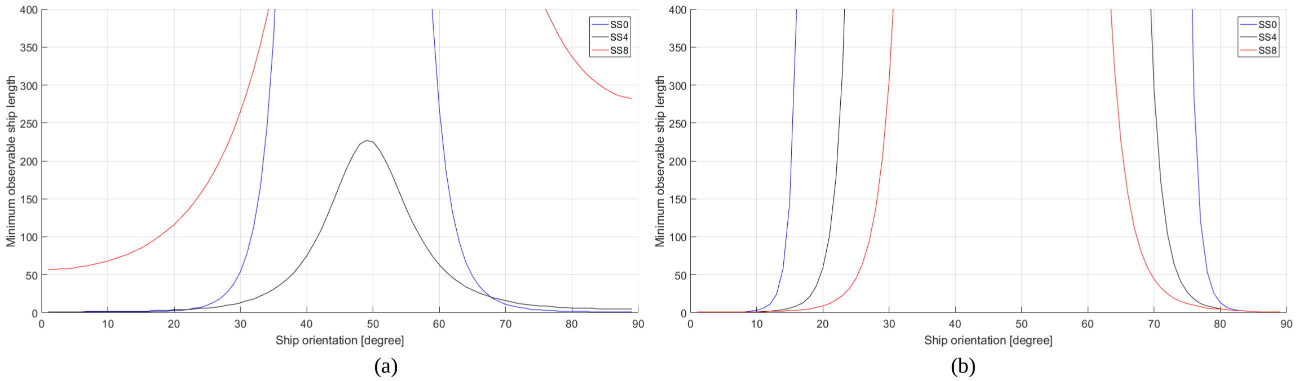


Fig. 4: Minimum ship length achieving SNCR greater than one in backscattering as a function of the ship orientation and for different sea states. (a) $\vartheta = 15°$, (b) $\vartheta = 30°$.